



Original article

Development of novel-nanobody-based lateral-flow immunochromatographic strip test for rapid detection of recombinant human interferon $\alpha 2b$



Xi Qin ^{a,1}, Maoqin Duan ^{a,1}, Dening Pei ^{a,1}, Jian Lin ^b, Lan Wang ^a, Peng Zhou ^b, Wenrong Yao ^a, Ying Guo ^a, Xiang Li ^a, Lei Tao ^a, Youxue Ding ^a, Lan Liu ^a, Yong Zhou ^a, Chuncui Jia ^a, Chunming Rao ^{a,*}, Junzhi Wang ^{a,c,**}

^a National Institutes for Food and Drug Control, Beijing, 100050, China

^b Synthetic and Functional Biomolecules Center, Peking University, Beijing, 100871, China

^c WHO Collaboration Centre for Biologicals Standardization and Evaluation, Beijing, 100050, China

ARTICLE INFO

Article history:

Received 5 July 2020

Received in revised form

25 May 2021

Accepted 5 July 2021

Available online 8 July 2021

Keywords:

Recombinant human interferon $\alpha 2b$

Nanobody

Phage display

Screening

Rapid test

ABSTRACT

Recombinant human interferon $\alpha 2b$ (rhIFN $\alpha 2b$) is widely used as an antiviral therapy agent for the treatment of hepatitis B and hepatitis C. The current identification test for rhIFN $\alpha 2b$ is complex. In this study, an anti-rhIFN $\alpha 2b$ nanobody was discovered and used for the development of a rapid lateral flow strip for the identification of rhIFN $\alpha 2b$. RhIFN $\alpha 2b$ was used to immunize an alpaca, which established a phage nanobody library. After five steps of enrichment, the nanobody I22, which specifically bound rhIFN $\alpha 2b$, was isolated and inserted into the prokaryotic expression vector pET28a. After subsequent purification, the physicochemical properties of the nanobody were determined. A semiquantitative detection and rapid identification assay of rhIFN $\alpha 2b$ was developed using this novel nanobody. To develop a rapid test, the nanobody I22 was coupled with a colloidal gold to produce lateral-flow test strips. The developed rhIFN $\alpha 2b$ detection assay had a limit of detection of 1 $\mu\text{g}/\text{mL}$. The isolation of I22 and successful construction of a lateral-flow immunochromatographic test strip demonstrated the feasibility of performing ligand-binding assays on a lateral-flow test strip using recombinant protein products. The principle of this novel assay is generally applicable for the rapid testing of other commercial products, with a great potential for routine use in detecting counterfeit recombinant protein products.

© 2021 The Authors. Published by Elsevier B.V. on behalf of Xi'an Jiaotong University. This is an open access article under the CC BY-NC-ND license (<http://creativecommons.org/licenses/by-nc-nd/4.0/>).

1. Introduction

Interferon (IFN), a protein with a broad-spectrum antiviral activity in allogeneic cells, was discovered by Isaacs et al. [1,2] in 1957. The recombinant human interferon $\alpha 2b$ (rhIFN $\alpha 2b$), which was approved for the first time by the United States Food and Drug Administration in 1986, is one of the earliest recombinant proteins used as a drug worldwide [3]. RhIFN $\alpha 2b$ is currently used as an

antiviral agent for treatment of hepatitis B and hepatitis C. In China, rhIFN $\alpha 2b$ has been used since 1994 to treat hepatitis and control the spread of the disease.

The identification test, one of the most important physicochemical tests applied to recombinant proteins, preliminarily determines known proteins. The identification test is required to be highly specific, repeatable, sensitive, simple, and rapid. Part III of the Chinese Pharmacopoeia (2020) states that identification tests are often performed using immunoblotting and dot immunobinding assays [4]. These methods require antibody reagents with high specificity and the test should be sensitive and repeatable with the antibody. Most commercial antibodies used for recombinant protein detection are polyclonal or monoclonal. The antibody affinity for the test article varies considerably among different manufacturers and batches, which may affect the reproducibility of the

Peer review under responsibility of Xi'an Jiaotong University.

* Corresponding author.

** Corresponding author. WHO Collaboration Centre for Biologicals Standardization and Evaluation, Beijing, 100050, China.

E-mail addresses: raocm@nifdc.org.cn (C. Rao), wangjz_nifdc2014@163.com (J. Wang).

¹ These authors contributed equally to this study.

<https://doi.org/10.1016/j.jpha.2021.07.003>

2095-1779/© 2021 The Authors. Published by Elsevier B.V. on behalf of Xi'an Jiaotong University. This is an open access article under the CC BY-NC-ND license (<http://creativecommons.org/licenses/by-nc-nd/4.0/>).

assays. The production of these antibodies is complex and expensive. In addition, monoclonal and polyclonal antibodies must be stored and transported at low temperatures, which hinders the development of rapid testing. Thus, an antibody with high specificity for the target recombinant protein is required to achieve the proper sensitivity and repeatability of the test. Such an antibody would also simplify the identity test, reduce the cost, and increase the efficiency.

In 1993, Hamers-Casterman et al. [5] identified heavy chain antibodies (HCABs) in camels. Clones of heavy chain variable regions are known as nanobodies or variable domain of heavy chain (VHH) antibodies [6,7]. Nanobodies have a molecular weight of 15 kDa (tenth of the weight of normal antibodies), diameter of 2.2 nm, and length of 4.8 nm [8,9]. Nanobodies are composed of only one heavy chain variable region and are the smallest fragments that bind antigens in the nature [10]. Nanobodies have several advantages over traditional antibodies, including high water solubility, excellent stability [11–13], accurate targeting [14,15], low immunogenicity [16], strong tissue penetration [17], simple production [17], controlled half-life, and high modifiability [18].

Thus, nanobodies are a promising substitute for monoclonal and polyclonal antibodies for the identification of recombinant proteins. In this study, we used rhIFN α 2b to immunize an alpaca. After five rounds of immunization, we extracted total ribonucleic acid (RNA) from the alpaca lymphocytes. The VHH region was amplified using nested polymerase chain reaction (PCR) and a phage vector was constructed. Using phage display techniques and five rounds of enrichment, we obtained a new anti-rhIFN α 2b nanobody, I22. After preliminary characterization of the physicochemical properties and functions of I22, we used this nanobody in a rapid test of rhIFN α 2b. Finally, we developed an enzyme-linked immunosorbent assay (ELISA) method for a semiquantitative rhIFN α 2b identification and colloidal gold test strip method for rapid rhIFN α 2b identification.

2. Materials and methods

2.1. Reagents

Freund's adjuvant was purchased from Sigma-Aldrich (Beijing, China). A human peripheral blood lymphatic extraction solution was obtained from Solarbio (Beijing, China). Trizol reagent and Pierce electrochemiluminescence (ECL) Western blotting substrate were purchased from Thermo Fisher (Beijing, China). Taq enzymes and plasmid extraction kits were purchased from Promega (Beijing, China). *Escherichia coli* TG1, gel extraction kits, endonuclease, and deoxyribonucleic acid (DNA) purification kits were obtained from Invitrogen (Beijing, China). T4 DNA ligase was purchased from NEB (Beijing, China). TMB LIQMID-1 COMPENT was obtained from AMRESCO (Beijing, China).

2.2. RhIFN α 2b and other cytokines

The national standard for rhIFN α 2b was preserved in our department. RhIFN α 2b (listed product approved for treatment of hepatitis B, hepatitis C, malignant melanoma, etc.) and other cytokines, including recombinant human granulocyte colony-stimulating factor (rhG-CSF, listed product, approved for treatment of chronic severe neutropenia, acute myeloid leukemia, etc.), recombinant human interleukin-2 (rhIL-2, listed product, approved for treatment of renal cancer, melanoma, etc.), recombinant human interferon α 2a (rhIFN α 2 α , listed product, approved for treatment of chronic hepatitis C, etc.), and recombinant human interferon α 1b (rhIFN α 1b, listed product, approved for treatment of chronic hepatitis B, hepatitis C, and hairy cell leukemia), were provided by different manufacturers.

2.3. Alpaca immunization

The research on alpaca was performed in accordance with protocols approved by the Institutional Animal Care and Use Committee of Peking University, China. For the first round of immunization, 600 μ g of rhIFN α 2b was dissolved in a mixed solution of 2 mL of phosphate-buffered saline (PBS) and 2 mL of Freund's adjuvant. This mixture was injected into nine different alpaca sites. The second immunization was performed 14 days later, when 300 μ g of rhIFN α 2b was dissolved in a mixed solution of 2 mL of PBS and 2 mL of Freund's adjuvant and injected as described above. The third immunization was identical to the second immunization and was performed two weeks later. The fourth and fifth immunizations were identical to the second immunization. The fourth immunization was performed seven days after the third, while the fifth immunization was performed seven days after the fourth.

2.4. Total RNA extraction from lymphocytes

After five rounds of immunization, 3 mL of blood from the alpaca was collected. The blood was mixed with 3 mL of PBS. 6 mL of the human peripheral blood lymphocyte extracting solution was added and centrifuged at 800 relative centrifugal force (RCF) at 4 °C for 11 min to collect suspended lymphocytes. The cells were washed with an equal volume of PBS and resuspended in 200 μ L of PBS. 1 mL of Trizol mixed with 240 μ L of chloroform were added to the cellular suspension. The mixture was centrifuged at 12,000 r/min at 4 °C for 15 min. The supernatant was then collected. Isopropanol was added into the supernatant. The mixture was incubated at room temperature for 10 min, and then centrifuged at 12,000 r/min at 4 °C for 15 min. The precipitate was retained, washed twice with 750 μ L of ethanol (75%), and then dried. Finally, the RNA was dissolved in 50 μ L of diethylpyrocarbonate-treated water.

2.5. Construction of a phage nanobody library

The extracted RNA was reverse-transcribed into complementary DNA. The VHH fragment was amplified using nested PCR. The first-round PCR primers were VH-LD (5'-CTTGGTGGTCTGGCTGC-3') and CH2-R (5'-GGTACGTGCTGTTGAAGTGTCC-3') [19], while the second-round PCR primers were VHH-shortR2 (5'-CGAGTGCCGCCGCGGGTCTTCGCTGTGGTGCG-3') and VHH-shortR1 (5'-CGAGTGCCGCCGCTTGTGGTTTTGGTGTCTTGGG-3') [19]. The amplified VHH fragment and pHEN1 vector were digested with NotI and SfiI. The digested fragments were added to 500 μ L of a connection system (5 μ g of pHEN1, 1.5 μ g of VHH, 3 μ L of T4 DNA ligase, 50 μ L of 10 \times T4 DNA ligase buffer, filled to 500 μ L with distilled water) at 16 °C for 12 h. The linked products were added to 15 competent *E. coli* TG1 cells (80 μ L/vial), electrically shocked at 1.8 kV, added into 500 μ L of a lysogeny broth (LB) culture medium, cultured at 37 °C for 2.5 h with shaking at 150 rpm, and cryopreserved.

2.6. Phage display

The TG1 bacterial solution (2.5 mL) was added into a 2 \times YT culture medium containing 3% glucose. The solution was cultured at 30 °C with shaking at 200 r/min until the optical density 600 (OD₆₀₀) reached 0.7. One milliliter of M13K07 was then added. The mixture was incubated at 37 °C for 30 min, followed by additional 2 h at 37 °C with shaking at 220 r/min. The bacterial cultures were centrifuged at 6,000 r/min for 5 min at 4 °C, resuspended in 20 mL of the 2 \times YT culture medium containing 3% glucose, and cultured overnight at 37 °C with shaking at 200 rpm. Bacterial cultures were centrifuged at 2,500 r/min for 20 min at 4 °C and the supernatants

were collected. The phages were spread on a plate to calculate the colony sizes and titers.

2.7. Liquid-phase screening

We used a magnetic-bead purification system to screen the phage display library using standard reagents and screening procedures. 27 μL of a 10 mM N-hydroxysuccinimidobiotin reagent solution (dissolved in dimethylsulfoxide) was added to 1 mL of 2 M rhIFN α 2b solution (dissolved in PBS). The reaction was incubated at room temperature for 30 min, followed by dialysis to remove unreacted biotin. Magnetic beads (labeled with streptavidin) were cleaned with 700 μL of PBS and then the labeled rhIFN α 2b was added for 30 min. After washing with PBS, the phage library was added. After binding for 30 min, the beads were collected and cleaned with 700 μL of PBS, PBS with Tween (PBST), and PBS three times to remove nonspecific binding phages. The bound phages were eluted with a glycine solution (pH 2.2). We used 100 μL of 1 M Tris-HCl (pH 8.0) to neutralize the screened eluate. The eluted phages were amplified and used for the next round of screening. This procedure was performed five times in total. Amplifications were performed as described in Section 2.6.

2.8. Construction, induced expression, and purification of the prokaryotic expression plasmid

The isolated nanobody sequence was amplified and end-modified by PCR with the primers 5'-CATGCCATGGGCCACCACCACCACCAGGTGCAGCTCGTGGAG-3' and 5'-CCGCTCGAGTGAGGAGACGGTGACCTG-3', and then inserted into the prokaryotic expression vector pET28a after digestion with NcoI and XhoI restriction enzymes. This vector was then transformed into *E. coli* BL21. Positive clones were selected and cultured in the LB medium. When the OD₆₀₀ of each culture reached 0.9, isopropyl β -D-thiogalactoside (IPTG) was added to obtain a final concentration of 0.8 mM. The culture was then transferred to a shaker and incubated at 16 °C for 12 h. After incubation, the culture was centrifuged at 7,000 r/min at 4 °C for 30 min. The precipitate was resuspended in PBS by sonication at a low temperature, and then recentrifuged. The supernatant was then collected and purified using a nickel column (K10324, TransGen Biotech, Beijing, China).

2.9. ELISA

100 μL of the rhIFN α 2b standard and rhIFN α 2b products were tested using 96-well plates. The plates were incubated overnight at 4 °C, and then sealed with 100 μL of 5% bovine serum albumin (BSA) at 37 °C for 1 h. After washing each plate five times with PBST, 100 μL of the 100 $\mu\text{g}/\text{mL}$ I22 antibody was added, which was then incubated for 1 h at 37 °C. After incubation, each plate was washed five times with PBST. 100 μL of anti-His-HRP antibody (1:1600; MAB050H, R&D Systems, Minneapolis, MN, USA) was then added. The plates were cultured at 37 °C for 1 h, and then washed five times with PBST. 100 μL of 3,3',5,5'-tetramethyl benzidine (TMB) LIQMID-1 COMPENT (XS12, Cygnus Technologies, Beijing, China) was added into each well, followed by incubation in dark for 30 min. Finally, 50 μL of 3 M H₂SO₄ was added to terminate the reaction. The OD of each well at 450 nm was then recorded.

2.10. Western blotting

After 4%–12% NuPAGE bis-tris gel electrophoresis (NP0321BOX, Invitrogen, Carlsbad, CA, USA), the membranes were transferred and sealed with 5% BSA for 30 min. The membranes were incubated with the primary antibody for 1 h, washed three times with PBST,

incubated with the secondary antibody for 1 h, washed with PBST three times, and then developed using a TMB color development solution or ECL solution.

2.11. Preparation of test strips using colloidal gold nanobody labeling

The nanobody was dialyzed with 10 mM of potassium phosphate buffer (pH 7.4) for 2 h. One milliliter of a colloidal gold (particle size: 40 nm, concentration: 1 mg/mL; HyperCyte, Beijing, China) was dissolved in 10 μL of 0.2 M potassium carbonate (pH adjusted to the isoelectric point (pI) of I22 + 0.2). 20 μg of the nanobody I22 was then added into the solution dropwise. This solution was mixed, and then allowed to stand for 40 min. 90 μL of 8% BSA was then added. The reaction was allowed to progress for 40 min. The mixture was then centrifuged at 14,000 r/min for 35 min at 4 °C. The precipitate was then washed six to eight times with PBS containing 1% BSA. After washing, the precipitate was redissolved in 600 μL of the colloidal gold solution and dried on a gold pad. The rhIFN α 2b standard was diluted with PBS to a concentration of 2 mg/mL. The anti-His antibody was diluted with PBS to 1 mg/mL. A nitrocellulose (NC) filter membrane was coated with 10 μL of the rhIFN α 2b standard or anti-His antibody and dried at room temperature. On the base-plate, the absorbent paper, NC membrane, gold pad, and sample chromatography pad were laid sequentially (in this order, from top to bottom). These layers were then cut into test strips with the width of 3.6 mm.

3. Results

3.1. Construction of the anti-rhIFN α 2b nanobody library

After the alpaca was immunized in five rounds with the rhIFN α 2b antigen, the serum immune titer in blood samples was measured seven days after each round of immunization. After the third round of immunization, the serum titer was significantly higher than that without immunization ($P < 0.001$; Fig. 1A). After the fifth round of immunization, the serum titer was 6.4×10^4 (detection after 1000 \times predilution). Peripheral blood lymphocytes were used to obtain the phage display library. We extracted RNA from lymphocytes in the serum obtained from the alpaca after the five rounds of immunization (Fig. 1B). After reverse transcription, the VHH fragment was amplified using nested PCR (Fig. 1C). This fragment was inserted into the pHEN1 vector, and then transferred into *E. coli* TG1 to obtain the rhIFN α 2b nanobody library. Colony detection and random PCR identification indicated that the library capacity was 2.74×10^8 , while the insertion efficiency was 98% (Fig. 1D). These levels were suitable for nanobody screening.

3.2. Nanobody screening

The nanobody was displayed on the phage surface using M13K07. The plaque test indicated that the recombinant phage titer was 3.1×10^{13} CFU/mL. Liquid-phase screening was then performed. The magnetic-bead-associated rhIFN α 2b protein was mixed with the nanobody phage display library, and then nonspecifically bound recombinant phages were removed by washing. The specifically bound recombinant phage was eluted, amplified, and used for the next round of screening. This procedure was performed five times; the concentrations of coated antigens were 100, 50, 20, 10, and 5 $\mu\text{g}/\text{mL}$, respectively. The single clone of the recombinant phage eluted after the last round of screening was selected and amplified as the primary antibody in an ELISA. In the ELISA screening, rhIFN α 2b was used as the antigen and anti-His

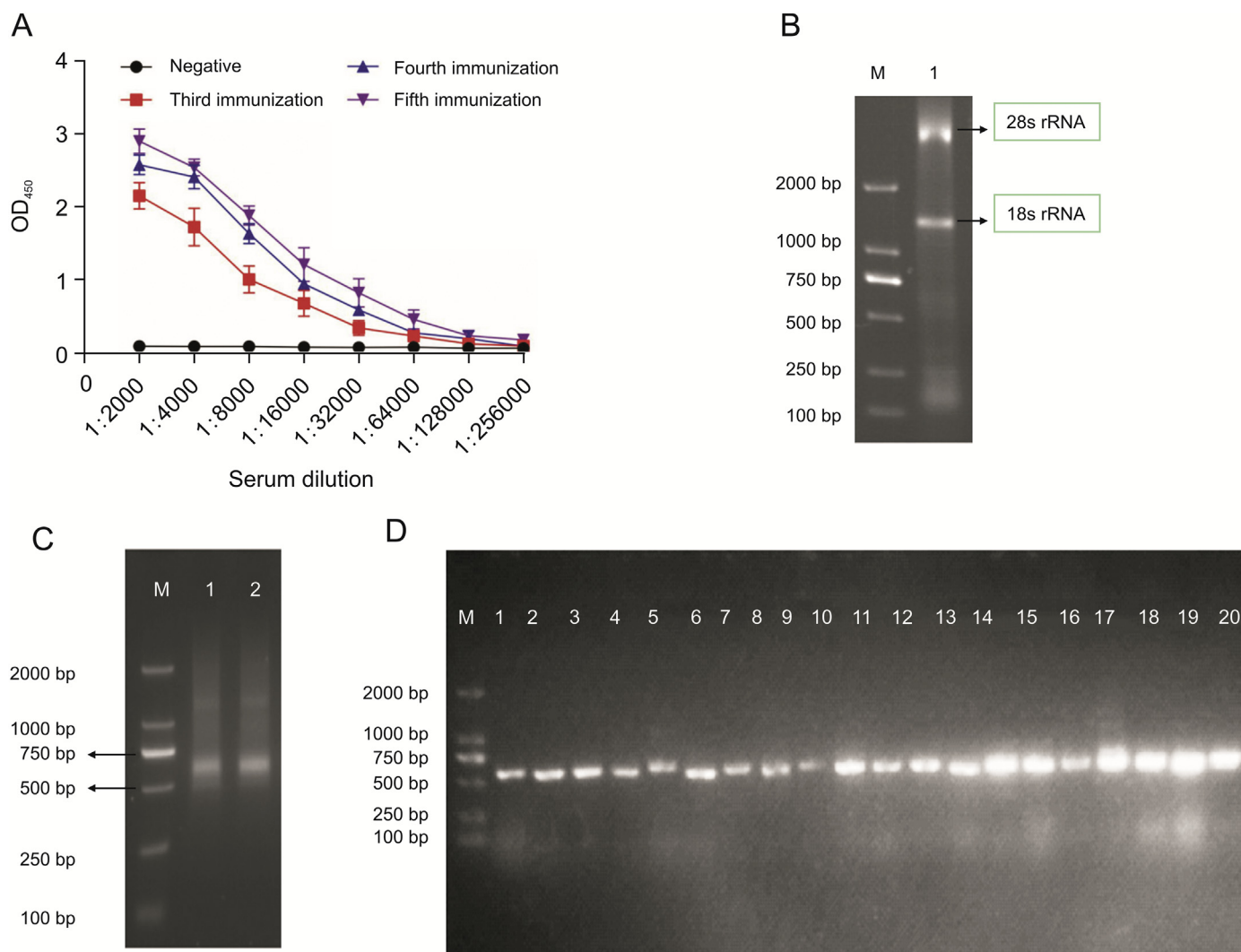


Fig. 1. Construction and identification of the phage nanobody library against rhIFN α 2b. (A) Detection of serum immune titers after the alpaca was immunized in five rounds with the rhIFN α 2b antigen. (B) Extraction of total RNA from lymphocytes. (C) Amplification of the VHH fragment (1 and 2: 2 PCR systems with the difference of extracted RNA template). (D) PCR identification of the anti-rhIFN α 2b nanobody library (1–20: 20 single clones) (M: marker).

antibody was used as the secondary antibody. After screening 20 single clones with ELISAs, two positive clones were identified (Fig. 2A). These two recombinant phages had identical DNA sequences (amino acid sequence: QVQLVESGGGLVQPGGSLRLSCVASG FTFSATMSWHRQAPGREREFVAMTSGGGMINYANSVKGRFTISRDNKNTVYLQMDSLKPEDTAVYYCHRLGTFHWGQGTQVTVSSLE; Fig. 2B) and were designated I22. I22 was used for Western blotting, where the I22 display phage was used as the primary antibody and the anti-His antibody was used as the secondary antibody (Fig. 2C). The nanobody I22 clearly identified rhIFN α 2b, as evidenced by the I22 band intensity increase with the rhIFN α 2b concentration.

3.3. Construction and expression purification of the prokaryotic expression plasmid

The His-labeled I22 proteins expressed in the supernatant were purified using nickel columns (Fig. 3A). A gray scan analysis indicated that the purity of the purified I22 protein was 100.0%. A Quick StartTM Bradford Protein Assay Kit (5000202; Bio-Rad, Hercules, CA, USA) was used to detect the protein content and calculate the I22 yield per liter (Fig. 3B). This experiment was performed three times. The average yield of I22 per liter of the bacterial solution was 45.7 mg.

3.4. Physicochemical properties of I22

The membranes were transferred to an N-terminal sequencer (PPSQ-53A; Shimadzu, Shanghai, China). The sequence of 16 amino acids at the N-terminal was GHHHHHHQVQLVESGG, which was consistent with the theoretical sequence of I22 (data not shown).

I22 was treated with dithiothreitol and the equipment was calibrated with a NaI calibration solution. Liquid chromatography-mass spectrometer (Xevo G2 Q-TOF; Waters, Milford, MA, USA) was used to carry out an intact mass analysis. The measured molecular weight of I22 was 14,226.80 Da, consistent with the theoretical molecular weight (14,226.77 Da; Fig. 4A).

The nanobody I22 was mixed (to yield a final concentration of 100 μ g/mL) with 1% methylcellulose, 8 M urea solution, amphoteric electrolyte 3–10, and two pI markers. After degassing, the solution was injected and analyzed with capillary isoelectric focusing (iCE3; ProteinSimple, Minneapolis, MN, USA). The pI of the I22 protein was 8.20 approximately (Fig. 4B).

3.5. Affinity between I22 and rhIFN α 2b

The binding force between I22 and rhIFN α 2b was measured with the Octet platform (Octet RED96; Goettingen, Germany).

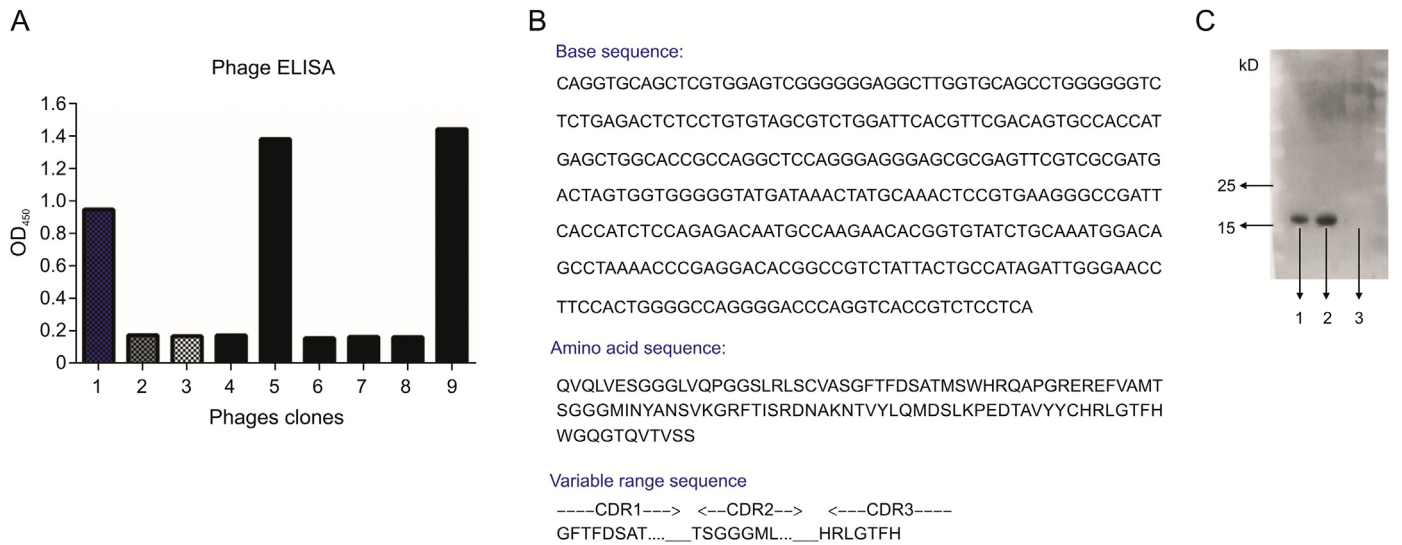


Fig. 2. Screening and identification of the nanobody. (A) Two positive clones were identified in 20 single clones with ELISAs. (B) Sequence of the isolated nanobody I22. (C) Verification of I22 by Western blotting (lane 1: 1 μg of rhIFN α 2b; lane 2: 2 μg of rhIFN α 2b; lane 3: HSA).

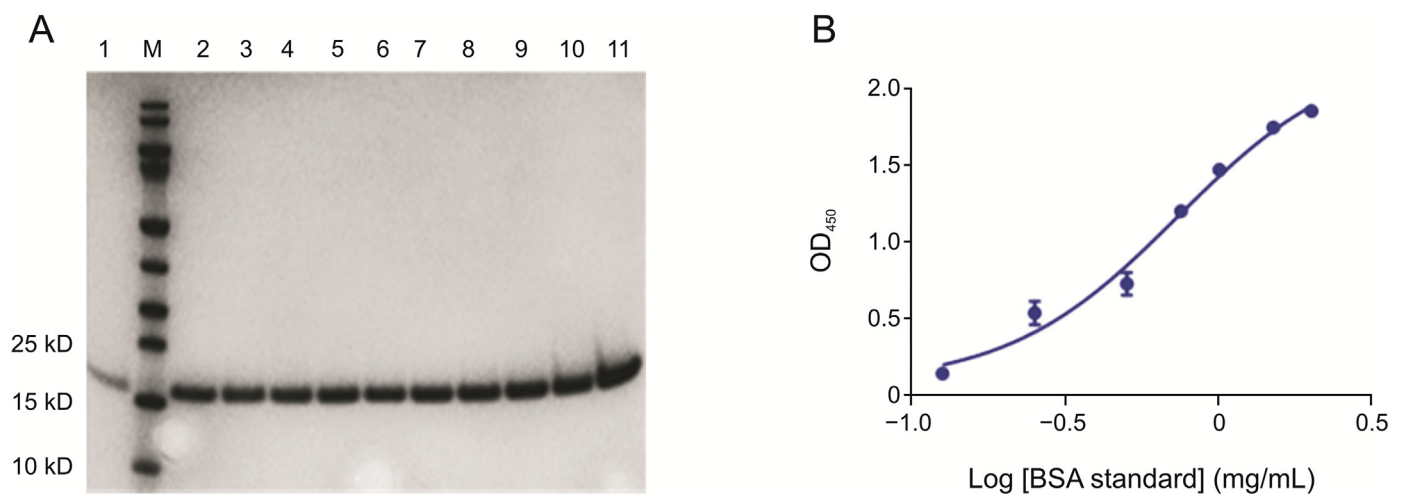


Fig. 3. Purification and yield of I22. (A) Electrophoresis of purified I22 (lanes 1–11: purified I22 and eluted for 1.5, 2, 2.5, 3, 3.5, 4, 4.5, 5, 5.5, and 6 min, respectively; lane M: marker). (B) Calculation of the I22 concentration using bovine serum albumin (BSA) as the standard ($R^2=0.98$).

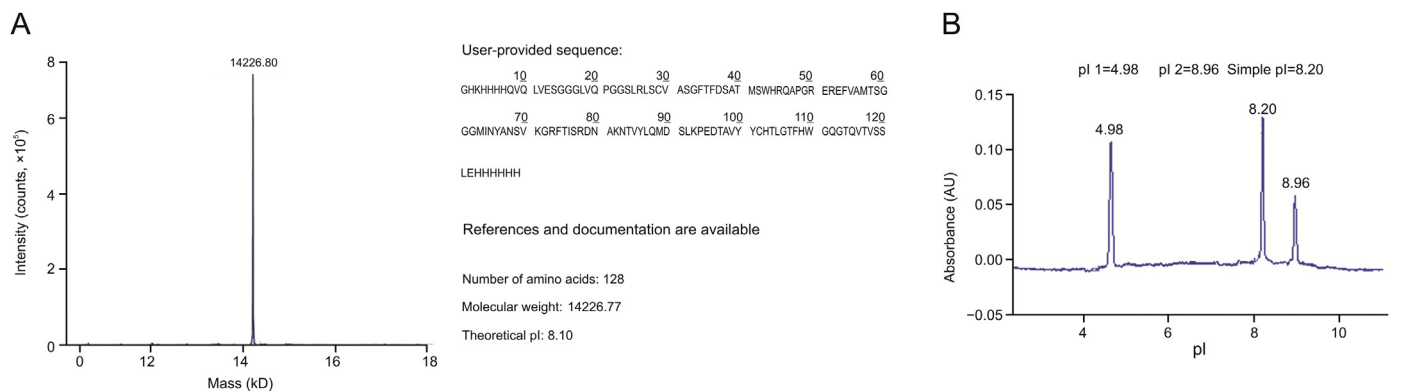


Fig. 4. Physicochemical properties of I22. (A) Deconvoluted mass spectrum of the I22 protein. (B) Capillary isoelectric focusing of I22 (analyte: 85% phosphoric acid solution; catholyte: 50% NaOH solution; low pI mark=4.98, high pI mark=8.96).

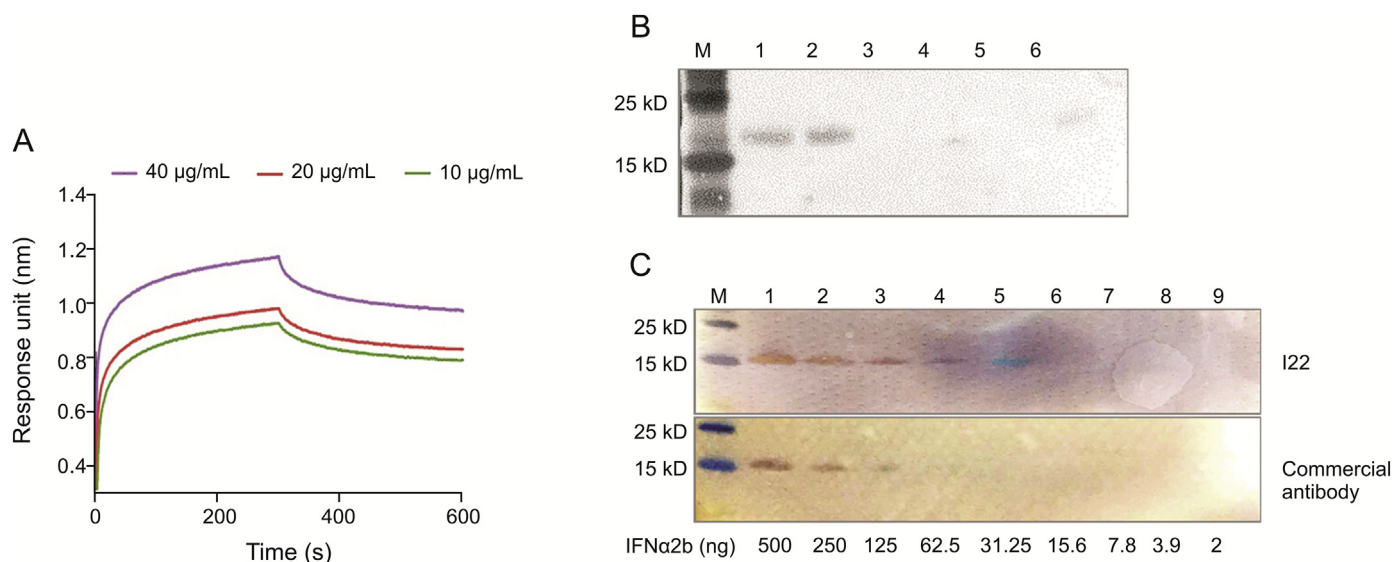


Fig. 5. Affinity between I22 and rhIFN α 2b. (A) 10 μ g/mL rhIFN α 2b product combined with 40, 20, or 10 μ g/mL nanobody I22. The samples were analyzed by following Octet procedures. (B) 10 μ g of the recombinant protein was detected after electrophoresis and membrane transfer, using 1 μ g/mL I22 as the primary antibody (lanes 1–6 are the rhIFN α 2b standard, rhIFN α 2b product, rhIFN α 1b product, rhG-CSF product, rhIL-2 product, and rhIFN α 2a product, respectively). (C) Comparison of I22 to a commercial antibody as primary antibodies in Western blotting to detect rhIFN 2b as the antigen (lanes 1–9 are rhIFN 2b standards with masses of 500, 250, 125, 62.5, 31.25, 15.6, 7.8, 3.9, and 2 ng, respectively; M: marker).

The dissociation curve was shown in Fig. 5A, and the equilibrium dissociation constant (K_D) value obtained by calculation was 2.06×10^{-9} M, suggesting that I22 had a high affinity for rhIFN α 2b.

The binding specificity between I22 and rhIFN α 2b was evaluated using Western blotting. I22 was used to detect the rhIFN α 2b standard, rhIFN α 2b product, rhIFN α 1b product, rhG-CSF product, rhIL-2 product, and rhIFN α 2a product (containing protective ingredients, e.g., human serum albumin (HSA), trehalose, etc.). I22 bound to rhIFN α 2b; the binding affinity was not decreased in the presence of the HSA (Fig. 5B). I22 also bound to rhIFN α 2a, but the binding affinity was lower than that of I22 and rhIFN α 2b.

The nanobody I22 and commercial anti-rhIFN α 2b monoclonal antibody (ab9386; Abcam, Cambridge, UK) were diluted to 1 μ g/mL and used to detect rhIFN α 2b in gradient dilutions. Two secondary antibodies, horseradish peroxidase (HRP)-labeled anti-His secondary antibody (R931-25; Thermo, Carlsbad, CA, USA) and HRP-labeled mouse secondary antibody (HS201; TransGen, Beijing, China), were used to compare the sensitivity of I22 and commercial anti-rhIFN α 2b monoclonal antibodies, respectively. TMB staining indicated that the limit of detection of I22 (at 1 μ g/mL) was 31.25 ng, while the limit of detection of the anti-rhIFN α 2b monoclonal antibody (at 1 μ g/mL) was 125 ng (Fig. 5C). Thus, the sensitivity of the nanobody I22 was not lower than that of the anti-rhIFN α 2b monoclonal antibody.

3.6. Semiquantitative detection of rhIFN α 2b using I22

Preliminary experiments indicated that the rhIFN α 2b binding to I22 increased with the I22 concentration in a dose-dependent manner (Fig. 6A). The diluted rhIFN α 2b standard and rhIFN α 2b samples were used to coat 96-well plates. An ELISA was then performed using 100 μ g/mL I22 as the primary antibody. Over three repetitions of the ELISA, the concentrations of the five rhIFN α 2b products were accurately and consistently measured (Figs. 6B and C).

3.7. Rapid identification of rhIFN α 2b using I22

After labeling with the colloidal gold, the I22 nanobody was used to construct the test strips (Fig. 7). The absence of red band on the quality control line indicates an invalid test strip. A red band on the quality control line and negative detection line indicate that rhIFN α 2b was not detected or that the rhIFN α 2b concentration was too low. A red band on the quality control line and absence of a detection line indicate that rhIFN α 2b was detected. At an rhIFN α 2b concentration of 1 μ g/mL, the test strip returned a positive result (Figs. 8A and S1). The rhIFN α 2b limit of detection for the test strip was 1 μ g/mL, as indicated by multiple tests. The whole test time only takes a few minutes.

Both liquid rhIFN α 2b products and dissolved powdered rhIFN α 2b products with different compositions were successfully detected with I22 colloidal gold test strips (Fig. 8B). The blank group was negative. This result indicates that the accessories in rhIFN α 2b products did not influence the test results. Thus, these strips can be used for the detection of conventional rhIFN α 2b products.

4. Discussion

Both solid-phase and liquid-phase screening methods use phages to screen antibody libraries. The operation of solid-phase screening is very simple [20]: the target is specifically bound and nonspecifically bound species are eluted. Liquid-phase screening uses a biotin–magnetic-bead system and streptavidin–target antigen to screen specific target proteins [21]. Liquid-phase magnetic-bead screening has numerous advantages, including specificity, stability, accuracy, and complete exposure of the antigen. Less antigen is required for liquid-phase screening than solid-phase screening [22,23]. In this study, we screened the antibody library using liquid-phase screening.

Nanobodies can be expressed using various expression systems [24–28]. Nanobodies, which are expressed with a high titer in prokaryotic cells, are inexpensive and simple to express and do not require posttranslational modifications. Therefore, *E. coli* was chosen to express the nanobody I22. Protein fragments tagged at

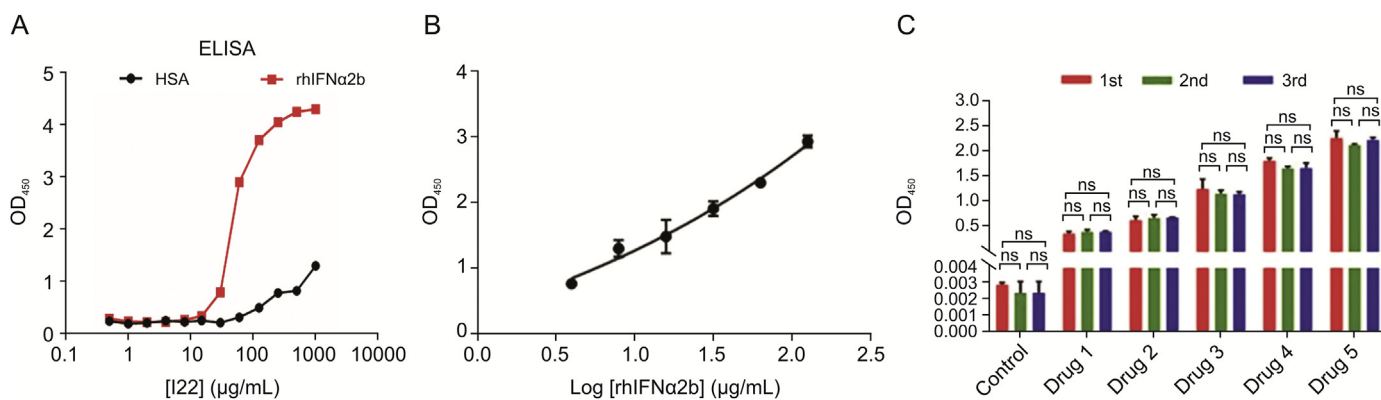


Fig. 6. Semiquantitative detection of rhIFN α 2b with I22. (A) The rhIFN α 2b binding to I22 increased with the I22 concentration in a dose-dependent manner. (B) Standard curve for the semiquantitative detection of rhIFN α 2b. (C) Statistical analysis of three repeated semiquantitative detection experiments using I22 to detect five rhIFN α 2b products (ns: no difference in statistics).

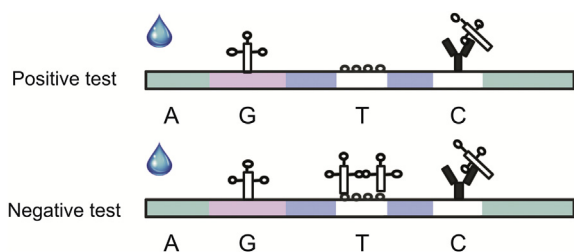


Fig. 7. Detection principle of the nanobody-coupled colloidal gold test strip. A: the detection area (loading area); G: the area containing the nanobody labeled with the colloidal gold; T: the detection line, coated with the rhIFN α 2b standard; and C: the quality control line, coated with the anti-His-labeled antibody.

the N- or C-terminal [29] are easy to use for the purification and detection of target proteins [30,31]. During the preparation of the nanobody I22, pET28a was used to add six His residues at the N- and C-terminals to increase the ease of purification. After the addition of His to these terminals, the nanobody still specifically binds the antigen rhIFN α 2b, with not lower binding sensitivity than that of the anti-rhIFN α 2b monoclonal antibody. Therefore, the His-labeling simplified the protein purification, increased the efficiency, and improved the I22 detection without reducing the I22 utility. In the comparison of the I22 and commercial anti-rhIFN α 2b antibodies, anti-His and antimouse antibodies were used, respectively, as secondary antibodies. These secondary antibodies were applied in excess to exclude the differences in affinity between the primary–secondary antibody pairs. The dilution ratio of the HRP-labeled anti-His secondary antibody was 1:500, while that of the HRP-labeled mouse secondary antibody was 1:200. (Fig. S2). Thus, the differences in binding affinity were equivalent to the differences in affinity between the primary antibodies to the rhIFN α 2b antigen. 45.7 mg of I22 was purified from 1 L of the bacterial solution. However, the typical expression level of the hybridoma-generated commercial monoclonal antibody is ~25 mg/L. Thus, I22 was not only more economically produced than the commercial monoclonal antibody [32], but also had a substantially larger yield.

RhIFN α 2a and rhIFN α 2b have lengths of 165 amino acids and differ at only two sites: AA23 is K in the rhIFN α 2a sequence and R in the rhIFN α 2b sequence, while AA112 is K in the rhIFN α 2a sequence and N in the rhIFN α 2b sequence. Thus, it is not surprising that the

specificity test indicated that I22 binds rhIFN α 2a, but with a lower affinity. After neutralization with I22, rhIFN α 2b did not affect its biological activity (Fig. S3). It was confirmed that I22 did not block the active site of rhIFN α 2b and that I22 was not the neutralizing antibody of rhIFN α 2b.

The binding between nanobodies and antigens is more stable than that between traditional antibodies and antigens. Even at high temperatures or extreme pHs, nanobodies stably bind antigens [33,34]. Furthermore, nanobodies are not prone to aggregation. The

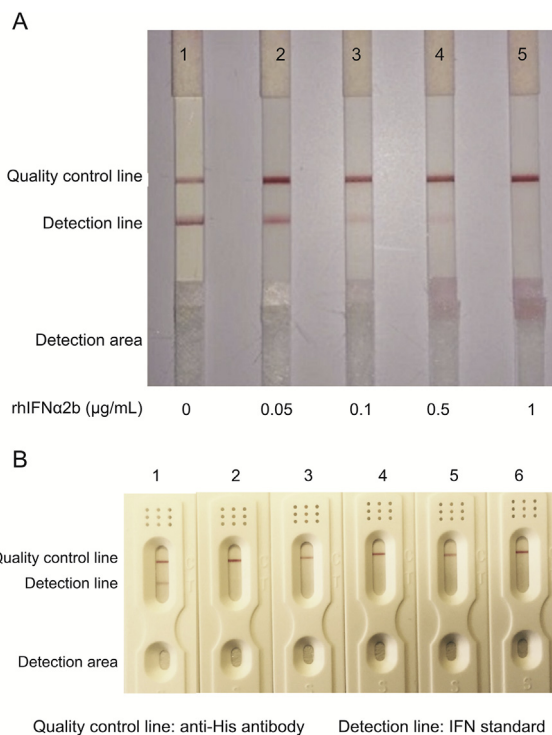


Fig. 8. Rapid detection of rhIFN α 2b using the developed paper strips. (A) The limit of detection of the rhIFN α 2b test strip was 1 μ g/mL. (B) Detection of different rhIFN α 2b product ingredients using test strips (1: water; 2: powder products of rhIFN α 2b from manufacturer A; 3: powder products of rhIFN α 2b from manufacturer B; 4: powder products of rhIFN α 2b from manufacturer C; 5: liquid products of rhIFN α 2b from manufacturer B; 6: liquid products of rhIFN α 2b from manufacturer C).

strong binding of nanobodies results from a specific bulge loop structure containing coupled disulfide bonds, which makes the molecule more stable. Thus, the nanobodies were also stable at room temperature.

The rhIFN α 2b products currently available in China include injections, injection powders, gels, and pastes. These strips can only be used to evaluate liquids or products in powder format that can be dissolved and applied to the strips, because the product needs to diffuse along the strip by capillary action; gels and pastes do not satisfy this requirement. Across all available injections and injection powders, the lowest rhIFN α 2b concentration is 10 μ g/mL. As the I22 colloidal gold-labeled test strips developed in this study offer a limit of detection of 1 μ g/mL, these strips would be suitable for the rapid test of available rhIFN α 2b products with liquid and powder formats. Owing to the advantages of nanobodies in reagent preservation, production, and cost, the lateral-flow immunochromatography assay using nanobodies has a high potential to replace traditional antibody-based ligand-binding assays for a rapid identification test of recombinant protein therapeutics.

5. Conclusions

An anti-rhIFN α 2b nanobody, I22, was discovered and developed by immune library establishment, molecular screening, expression cloning, and purification. Western blot experiments indicated that I22 is more sensitive, inexpensive, and stable than traditional antibodies. This novel nanobody I22 fits ELISAs, enabling the development of a sensitive and accurate method for semiquantitative detection of rhIFN α 2b. The coupling of the nanobody I22 with the colloidal gold provided a lateral-flow immunochromatographic test strip, which enabled a limit of detection of 1 μ g/mL for rapid identification tests and quality control. Notably, the limit of detection can be further improved through rigorous optimization. The operation time of rhIFN α 2b identification was shortened from two days (using an immunoassay) to a few minutes (using I22 colloidal gold test strip), and this test could meet the needs for rapid detection of this family of recombinant protein products on the market and provide a good foundation for improving the efficiency of market counterfeit detection and carrying out rapid detection in an all-round manner in the future.

CRediT author statement

Xi Qin: Methodology, Software, Validation, Formal analysis, Investigation, Data curation, Writing - Original draft preparation, Reviewing and Editing, Visualization, Conceptualization; **Maoqin Duan:** Methodology, Software, Validation, Formal analysis, Investigation, Data curation, Writing - Original draft preparation; **Dening Pei:** Methodology, Software, Validation, Formal analysis, Investigation, Data curation, Writing - Original draft preparation; **Jian Lin:** Methodology, Software, Visualization, Resources; **Lan Wang:** Methodology, Validation, Formal analysis, Investigation; **Peng Zhou:** Methodology, Software, Visualization; **Wenrong Yao:** Methodology, Validation, Formal analysis, Investigation; **Ying Guo:** Methodology, Validation, Formal analysis; **Xiang Li:** Methodology, Validation, Formal analysis; **Lei Tao:** Methodology, Validation, Formal analysis; **Youxue Ding:** Validation, Formal analysis, Investigation; **Lan Liu:** Validation, Formal analysis, Investigation; **Yong Zhou:** Validation, Formal analysis, Investigation; **Chuncui Jia:** Software, Visualization; **Chunming Rao** and **Junzhi Wang:** Conceptualization, Investigation, Resources, Supervision.

Declaration of competing interest

The authors declare that there are no conflicts of interest.

Acknowledgments

Financial support was provided by the National Science and Technology Major Project (Grant No.: 2015ZX09501008). The fund agency did not participate in the study's design, data collection and analysis, decision to publish, and preparation of the manuscript. We would like to thank Dr. Weijun Ma from the Shanghai Institutes for Biological Sciences for the provision of the vector Rphen1 and helper phages.

Appendix A. Supplementary data

Supplementary data to this article can be found online at <https://doi.org/10.1016/j.jpha.2021.07.003>.

References

- [1] A. Isaacs, J. Lindenmann, R.C. Valentine, Virus interference. II. Some properties of interferon, *Proc. R. Soc. Lond. B. Biol. Sci.* 147 (1957) 268–273.
- [2] A. Isaacs, J. Lindenmann, Virus interference. I. The interferon, *Proc. R. Soc. Lond. B. Biol. Sci.* 147 (1957) 258–267.
- [3] J.Z. Wang, Research, Development and Quality Control of Biopharmaceuticals, third ed., Science Press, Beijing, 2018, pp. 467–483.
- [4] Chinese Pharmacopoeia Commission, Pharmacopoeia of the People's Republic of China (Part III), 2020 edition, China Medical Science Press, Beijing, 2020, pp. 309–320.
- [5] C. Hamers-Casterman, T. Atarhouch, S. Muyldermans, et al., Naturally occurring antibodies devoid of light chains, *Nature* 363 (1993) 446–448.
- [6] C. Li, Z. Tang, Z. Hu, et al., Natural single-domain antibody-nanobody: a novel concept in the antibody field, *J. Biomed. Nanotechnol.* 14 (2018) 1–19.
- [7] P. Bannas, J. Hambach, F. Koch-Nolte, Nanobodies and nanobody-based human heavy chain antibodies as antitumor therapeutics, *Front. Immunol.* 8 (2017), 1603.
- [8] S. Muyldermans, T.N. Baral, V.C. Retamozzo, et al., Camelid immunoglobulins and nanobody technology, *Vet. Immunol. Immunopathol.* 128 (2009) 178–183.
- [9] L.S. Mitchell, L.J. Colwell, Comparative analysis of nanobody sequence and structure data, *Proteins* 86 (2018) 697–706.
- [10] M. Yamagata, J.R. Sanes, Reporter-nanobody fusions (RANbodies) as versatile, small, sensitive immunohistochemical reagents, *Proc. Natl. Acad. Sci. U S A* 115 (2018) 2126–2131.
- [11] M. Dumoulin, K. Conrath, A. Van Meirhaeghe, et al., Single-domain antibody fragments with high conformational stability, *Protein Sci.* 11 (2002) 500–515.
- [12] S. Muyldermans, Nanobodies: natural single-domain antibodies, *Annu. Rev. Biochem.* 82 (2013) 775–797.
- [13] R.H. Van der Linden, L.G. Frenken, B. de Geus, et al., Comparison of physical chemical properties of llama VHH antibody fragments and mouse monoclonal antibodies, *Biochim. Biophys. Acta* 1431 (1999) 37–46.
- [14] B. Stijlemans, K. Conrath, V. Cortez-Retamozo, et al., Efficient targeting of conserved cryptic epitopes of infectious agents by single-domain antibodies. African trypanosomes as paradigm, *J. Biol. Chem.* 279 (2004) 1256–1261.
- [15] P.D. Skottrup, Structural insights into a high affinity nanobody: antigen complex by homology modelling, *J. Mol. Graph. Model.* 76 (2017) 305–312.
- [16] V. Cortez-Retamozo, N. Backmann, P.D. Senter, et al., Efficient cancer therapy with a nanobody-based conjugate, *Cancer Res.* 64 (2004) 2853–2857.
- [17] V. Cortez-Retamozo, M. Lauwereys, Gh G. Hassanzadeh, et al., Efficient tumor targeting by single-domain antibody fragments of camels, *Int. J. Cancer* 98 (2002) 456–462.
- [18] D. Pan, G.H. Li, H.Z. Hu, et al., Direct immunoassay for facile and sensitive detection of small molecule aflatoxin B1 based on nanobody, *Chemistry* 24 (2018) 9869–9876.
- [19] D.R. Maass, J. Sepulveda, A. Pernthaner, et al., Alpaca (*Lama pacos*) as a convenient source of recombinant camelid heavy chain antibodies (VHHs), *J. Immunol. Methods* 324 (2007) 13–25.
- [20] L. Aujame, F. Geoffroy, R. Sodoyer, High affinity human antibodies by phage display, *Hum. Antibodies* 8 (1997) 155–168.
- [21] M. Zhu, X. Gong, Y. Hu, et al., Streptavidin-biotin-based directional double Nanobody sandwich ELISA for clinical rapid and sensitive detection of influenza H5N1, *J. Transl. Med.* 12 (2014), 352.
- [22] N. Kobayashi, T. Karibe, J. Goto, Dissociation-independent selection of high-affinity anti-hapten phage antibodies using cleavable biotin-conjugated haptens, *Anal. Biochem.* 347 (2005) 287–296.
- [23] A. Pini, C. Ricci, L. Bracci, Phage display and colony filter screening for high-throughput selection of antibody libraries, *Comb. Chem. High Throughput Screen.* 5 (2002) 503–510.

- [24] R. Baghban, S.L. Gargari, M. Rajabibazl, et al., Camelid-derived heavy-chain nanobody against *Clostridium botulinum* neurotoxin E in *Pichia pastoris*, *Bio-technol. Appl. Biochem.* 63 (2016) 200–205.
- [25] C. Hemmer, S. Djennane, L. Ackerer, et al., Nanobody-mediated resistance to *Grapevine fanleaf* virus in plants, *Plant Biotechnol. J.* 16 (2018) 660–671.
- [26] M. Behdani, S. Zeinali, M. Karimipour, et al., Development of VEGFR2-specific nanobody *Pseudomonas* exotoxin A conjugated to provide efficient inhibition of tumor cell growth, *N. Biotechnol.* 30 (2013) 205–209.
- [27] P. Schotte, I. Dewerte, M. De Groeve, et al., *Pichia astoris* Mut^S strains are prone to misincorporation of *O*-methyl-L-homoserine at methionine residues when methanol is used as the sole carbon source, *Microb. Cell Fact.* 15 (2016), 98.
- [28] J.L. Liu, D. Zabetakis, E.R. Goldman, et al., Selection and characterization of single domain antibodies against human CD20, *Mol. Immunol.* 78 (2016) 146–154.
- [29] R.C. Stevens, Design of high-throughput methods of protein production for structure biology, *Structure* 8 (2000) R177–R185.
- [30] D.S. Waugh, Making the most of affinity tags, *Trends Biotechnol.* 23 (2005) 316–320.
- [31] K. Terpe, Overview of tag protein fusion: from molecular and biochemical fundamentals to commercial systems, *Appl. Microbiol. Biotechnol.* 60 (2003) 523–533.
- [32] E. Soler, L.M. Houdebine, Preparation of recombinant vaccines, *Biotechnol. Annu. Rev.* 13 (2007) 65–94.
- [33] P. Kunz, K. Zinner, N. Mücke, et al., The structural basis of nanobody unfolding reversibility and thermoresistance, *Sci. Rep.* 8 (2018), 7934.
- [34] Y. Wang, Z. Fan, L. Shao, et al., Nanobody-derived nanobiotechnology tool kits for diverse biomedical and biotechnology applications, *Int. J. Nanomedicine* 11 (2016) 3287–3303.